Tellus (2003), 55B, 270–289
Printed in UK. All rights reserved

TELLUS
ISSN 0280–6509

Estimating regional terrestrial carbon fluxes for the Australian continent using a multiple-constraint approach

I. Using remotely sensed data and ecological observations of net primary production

By YING PING WANG[1]* and DAMIAN J. BARRETT[2], [1]*CSIRO Atmospheric Research, Private Bag 1, Aspendale, Victoria 3195, Australia;* [2]*CSIRO Plant Industry, GPO Box 1600, ACT 2601, Australia and Cooperative Research Centre for Greenhouse Accounting, GPO Box 475 Canberra, ACT, 2601, Australia*

(Manuscript received 11 February 2002; in final form 30 September 2002)

ABSTRACT

We have developed a modelling framework that synthesizes various types of field measurements at different spatial and temporal scales. We used this modelling framework to estimate monthly means and their standard deviations of gross photosynthesis, total ecosystem production, net primary production (NPP) and net ecosystem production (NEP) for eight regions of the Australian continent between 1990 and 1998. Annual mean NPP of the Australian continent varied between 800 and 1100 Mt C yr^{-1} between 1990 and 1998, with a coefficient of variation that is defined as the ratio of standard deviation and mean between 0.24 and 0.34. The seasonal variation of NPP for the whole continent varied between 50 and 110 Mt C $month^{-1}$ with two maxima, one in the autumn and another in the spring. NEP was most negative in the winter (a carbon sink) and was most positive (a carbon source) in the summer. However, the coefficient of variation of monthly mean NEP was very large (> 4), and consequently confidence in the predicted net carbon fluxes for any month in the period 1990–1998 for the whole continent was very low. A companion paper will apply atmospheric inverse technique to measurements of CO_2 concentration to further constrain the continental carbon cycle and reduce uncertainty in estimated mean monthly carbon fluxes.

1. Introduction

Net primary production, or NPP, is the difference between gross photosynthesis and plant respiration over a time, and net ecosystem production, or NEP, is the difference between soil respiration and NPP over time. Mean global NPP of the terrestrial biosphere is estimated to be about 54 Gt C yr^{-1} (Field et al., 1995), but a recent comparison of simulation results by 16 different terrestrial ecosystem models found that estimated global terrestrial NPP varied between 44 and 66 Gt C yr^{-1}(Cramer et al., 1999), and that significant differences existed between different models in their predicted spatial and temporal variations of NPP. Thus, spatially explicit estimates of regional NPP remain quite uncertain. For the Australian continent, estimated total NPP varies between 1.0 and 3.2 Gt C yr^{-1} using process-based terrestrial ecosystem models (Gifford et al., 1992; Kirschbaum, 1999a; Raupach et al., 2001; Roderick et al., 2001). Since annual NEP is at least one order of magnitude smaller than NPP, and measurements of NEP are significantly fewer than those of NPP in Australia, the estimate of NEP of the Australian continent using those process-based models would be even less certain than that of NPP. Therefore development of methodologies to reduce this uncertainty is urgently needed.

It is not possible to measure the NPP or NEP of the whole Australian continent directly. The "bottom-up"

*Corresponding author.
e-mail: yingping.wang@csiro.au

or "top-down" approaches can be used instead, but each has problems. The bottom-up approach uses statistical or process-based models to calculate NPP and NEP. These models are usually developed using field measurements of NPP at the plot scale (about 10^4 m^2), and are used to estimate NPP or NEP of the Australian continent using spatially explicit information about the vegetation and soil (Barrett, 2001; Kirschbaum, 1999b). The advantages of bottom-up approaches are: (1) they include our current understanding about important ecosystem processes that control the exchange of CO_2 between the land surface and the atmosphere, such as the nexus between carbon uptake and water use by plants through stomata, which provide an important physiological constraint on the potential carbon uptake by a terrestrial ecosystem in a given climatic condition; (2) they can be calibrated using physiological and ecological measurements, most of which are made at different spatial or temporal scales. So far most measurements have been made at very fine spatial scales and a limited number of sites; (3) they can be used to estimate the spatial and temporal variation of net carbon exchange between the terrestrial biosphere and atmosphere at fine spatial and temporal scales if the inputs to the model are also available at those fine spatial and temporal scales; and (4) they can be used to predict the response of NPP or NEP under future climate conditions, provided they are adequately calibrated. The disadvantage of this approach is that not all knowledge at the process level is included in statistical models. Furthermore, the limited number of field observations and gaps in spatially explicit datasets may lead to biased predictions. Extrapolation of bottom-up models to large scales can also be problematic without extensive data coverage to constrain the model prediction at large scales. Estimates of NPP or NEP of the Australian continent using bottom-up approaches cannot yet be verified directly because direct measurements of NPP or NEP at the continental scale are currently not available.

The top-down approach estimates regional carbon fluxes by applying inverse techniques to the measurements of atmospheric CO_2 concentrations at different locations in the world. The advantage is that it can be applied to the measurements of atmospheric CO_2 concentrations at a limited number of locations to infer regional or global carbon fluxes because of the mixing power of the atmosphere (such as Tans et al., 1990; Biraud et al., 2000). The disadvantage of the inverse technique is that the atmospheric inversion using measurements of atmospheric CO_2 concentrations alone cannot resolve the spatial distribution of terrestrial carbon fluxes very well because of the uneven distribution of the measurement stations and coarse spatial resolution of atmospheric transport models used in the inversion. Bayesian inversion has been used in many global inversion studies, and requires the prior estimates of the mean and standard deviation of the mean (SD) of carbon fluxes, which can have significant influences on the inversion estimates. Therefore reasonable prior estimates can be important in Bayesian inversion. In this study we combine the two approaches, and use a process-based model, the CSIRO Biosphere Model (CBM) (Kowalczyk et al., 1994; Raupach, 1998; Wang and Leuning, 1998) to provide prior estimates of the mean and SD of monthly carbon fluxes and their seasonal variations for eight land regions of the Australian continent.

One of the key assumptions in this paper is that all terrestrial ecosystems are at steady-state, or their NEPs integrated over 9 yr are equal to zero. This assumption is unlikely to be true everywhere, but a reasonably accurate and the simplest one for most Australian terrestrial ecosystems for which there is insufficient information available for us to calculate gross photosynthesis, respiration and net carbon exchange. The most recent global carbon budget (IPCC, 1996) shows that the net carbon uptake by global terrestrial ecosystems is less than 4% of its total NPP, therefore annual mean global NPP is roughly equal to mean heterotrophic soil respiration, and global annual NEP is close to zero (IPCC, 1996). A recent study also has found that the ratio annual NPP/GPP is about half as much as gross primary production, or GPP for many ecosystems (Waring et al., 1997 and therein). When an ecosystem is not at steady state, annual NEP can be strongly negative (a sink), such as a young forest, or strongly positive (a source) such as for disturbed ecosystems. Many terrestrial ecosystems in Australia are probably at quasi-steady state, with their NEP being at least one order of magnitude smaller than NPP; it is, however, difficult to ascertain the exact state of the carbon dynamics of all terrestrial ecosystems because of the lack of measurements. The steady-state assumption allows us to calculate the carbon fluxes (gross photosynthesis, plant and soil respiration) using CBM from the estimates of NPP for steady-state terrestrial ecosystems, and estimates of carbon fluxes including NPP and NEP for non-steady-state terrestrial ecosystems will be obtained by applying Bayesian synthesis inversion to the measurements of surface atmospheric CO_2 concentration at Cape Grim, in north-west

Tasmania, Australia, and reported in the companion paper (Wang and McGregor, 2003).

This paper is organized as follows. Section 2 describes the methods used in parameterizing CBM and estimating the mean and SD of monthly carbon fluxes and section 3 describes the data (spatially explicit canopy green area index that is defined as the total area index of all green plant organs, estimates of NPP at 75 km by 75 km resolution for the Australian continent, and meteorological inputs to CBM). The results and discussion follow.

2. Methods

This section describes the relationship between different fluxes and methods used for calculating the mean and SD of monthly carbon fluxes for 1990 to 1998 from each of the eight land regions in Australia.

Our methods involve three models, VAST1.0 and CBM, and the error model relating the SD of annual mean NPP to the SD of monthly carbon fluxes for all land points in Australia. CBM has been described elsewhere (Wang and Leuning, 1998; Wang et al. 2001); both VAST1.0 and the error model will be described in the next two subsections. While VAST1.0 provides estimates of the mean and SD of annual NPP of the Australian continent at 5 km by 5 km spatial resolution (long-time and fine-spatial scale), CBM calculates the hourly fluxes of canopy photosynthesis, plant and soil respiration for the Australian continent at 75 km by 75 km spatial resolution because the analysed meteorological data are only available at the coarse spatial resolution (short-time and coarse-spatial scale). The advantage of VAST1.0 is that it was developed using field measurements of NPP and the disadvantage is that the temporal resolution of the estimated carbon fluxes is too coarse for atmospheric inversion, whereas CBM can be used to calculate hourly carbon fluxes, but estimating key model parameters is difficult without direct field measurements. The advantage of the approach developed here is that we combine different types of information in the inversion process to reduce uncertainty in estimated C-fluxes. In this study, we estimated the three key parameters in CBM using the predicted NPP from VAST1.0.

To make use of the merits of both VAST1.0 model and CBM, we estimated the mean and SD of monthly carbon fluxes in four steps. The first step is to estimate the mean and SD of annual NPP for every 5 km by 5 km grid cell of the Australian continent using VAST1.0 and 183 field measurements of NPP as described later (see section 2.2). The second step is to scale the mean and SD of annual NPP up to the 75 km by 75 km grid cell resolution used by CBM using the estimates of mean NPP by VAST1.0 and the SD of monthly NPP. The correct scaling of the error is achieved using the error model (see section 2.3). The third step is to use CBM and the estimate of mean annual NPP from step 2 to estimate three key parameters: the maximum canopy potential electron transport rate (J_{max}), non-leaf plant respiration rate at 20 °C (r_p) and soil respiration rate at 20 °C without soil water limiting (r_s) for every 75 km by 75 km grid cell of the Australian continent (section 2.4). The three key parameters in CBM are estimated by fitting the estimates of annual NPP calculated by CBM to the means of annual NPP scaled up from VAST1.0 for every 75 km by 75 km grid cell from step 2. The fourth step is to use CBM with the spatially explicit estimates of three key parameters to calculate the mean monthly carbon fluxes for the period 1990 to 1998 for every 75 km by 75 km grid cell of the Australian continent (see section 2.5). The SD of the mean monthly carbon flux is calculated from the estimate of SD of mean monthly NPP (section 2.3).

2.1. Key equations and definitions

In this study, we denote the vertical flux from land surface to the atmosphere as positive. Using CBM, we calculate the carbon fluxes of gross photosynthesis and plant and soil respiration separately.

The instantaneous biotic net carbon exchange between the land surface and the atmosphere, P_e, is calculated as the sum of canopy photosynthesis (P_g) and total respiration (R_t). That is

$$P_e = P_g + R_t \tag{1}$$

where P_g is calculated as

$$P_g = -V_c \left(1 - \frac{\Gamma^*}{C_i}\right). \tag{2}$$

Here V_c is the carboxylation rate as calculated using the photosynthesis model of Farquhar and von Caemmerer (1982), Γ^* is the CO_2 compensation point when day respiration is zero, and is the intercellular CO_2 concentration at which CO_2 evolved from photorespiration is equal to CO_2 fixed by carboxylation, and C_i is the intercellular CO_2 concentration. Calculation of V_c requires estimation of three physiological parameters, the maximum carboxylation rate (V_{cmax}), maximum potential electron transport rate (J_{max}) and the effective

Micahelis–Menten constant for Rubisco carboxylase (K_m). Potential electron transport rate represents the rate when neither final acceptor nor pH gradient across the thylakoid membrane limits the electron transport. The parameter K_m is related to the specific activity of Rubisco carboxylase and is calculated using the equation provided by Leuning (1990). A close correlation between V_{cmax} and J_{max} for many plant species has been found (Wullschledger, 1993), and the ratio of J_{max}/V_{cmax} was about 2.7 at a leaf temperature of 20 °C for C3 plants (Leuning, 1998). J_{max} is related to the maximum rate of potential electron transport of leaves at the top of the canopy, j_{max}, by

$$J_{max} = \frac{[1 - \exp(-k_n L)] j_{max}}{k_n} \quad (3)$$

where k_n is an empirical constant (=0.73 in this study). Sensitivity studies have shown that P_g is relatively insensitive to k_n for a given amount of canopy nitrogen (Leuning et al., 1995), and L is canopy green area index.

The total ecosystem respiration, R_t, is

$$R_t = R_f + R_p + R_s \quad (4)$$

where R_f is leaf respiration rate, R_p is non-leaf plant autotrophic respiration, and R_s is soil heterotrophic respiration. Total autotrophic respiration, R_a is calculated as $R_f + R_p$.

Non-leaf plant tissue (R_p) and soil respiration (R_s) rates are calculated as (Wang et al., 2001)

$$R_p = r_p \exp[0.069(T_f - 20)], \quad (5)$$

$$R_s = r_s f_T f_W, \quad (6)$$

where r_p and r_s are respiration rates of non-leaf plant tissue and soil at 20 °C and optimal soil moisture, T_f is leaf temperature (in °C), and f_T and f_W describe relative changes in soil respiration with variation in soil temperature and soil water content (Wang et al., 2001).

We also define gross photosynthesis ($P_{g,t}$) and net ecosystem production (NEP, $P_{e,t}$) over time t in the following way:

$$P_{g,t} = \int_t P_g dt \qquad t = \text{d, m or y} \quad (7)$$

$$P_{n,t} = P_{g,t} + R_{f,t} + R_{p,t} \qquad t = \text{d, m or y} \quad (8)$$

$$P_{e,t} = P_{g,t} + R_{f,t} + R_{p,t} + R_{s,t} \qquad t = \text{d, m or y} \quad (9)$$

where t is time, and is assigned d for day, m for month and y for year. Following convention, we defined the GPP, NPP and NEP as $-P_g$, $-P_n$ and $-P_e$, respectively, therefore both GPP and NPP are positive.

We also denote $\overline{P_{g,y}}$, $\overline{P_{n,y}}$, $\overline{P_{e,y}}$, $\overline{R_{a,y}}$ and $\overline{R_{s,y}}$ as the annual mean $P_{g,y}$, $P_{n,y}$, $P_{e,y}$ $R_{a,y}$ and $R_{s,y}$ averaged over several years for ecosystems approximately at steady state. We denote σ as the SD of the mean. For example, $\sigma_{n,y}$ denotes the SD of the annual mean NPP, $P_{n,y}$.

2.2. *Estimating the mean and standard deviation of net primary productivity at 5 km by 5 km spatial resolution for the Australian continent using VAST1.0*

We calibrated VAST1.0 using the data compiled by Barrett (2001). The data consist of 183 measurements of above-ground NPP, and the associated data of annual mean rainfall, air temperature, soil nutrient status and vegetation types. The calibrated VAST1.0 was used to estimate the mean and SD of the annual NPP for every 5 km by 5 km grid cell of the Australian continent.

Total net primary productivity in VAST1.0, $P_{n,y}$, (g C m^{-2} yr^{-1}) is the sum of the productivity of all plant tissues, above-ground fine tissue biomass ($P_{n,ya}$), below-ground fine tissues ($P_{n,yb}$), and above-ground coarse tissues ($P_{n,yc}$). That is

$$P_{n,y} = P_{n,ya} + P_{n,yb} + P_{n,yc} \quad (10)$$

where log-transformed above-ground fine tissue NPP was predicted by

$$\ln(P_{n,ya}) = \beta_0 + \beta_1 \ln(x_R), \quad (11)$$

where x_R is mean annual rainfall (mm) and β_0 and β_1 are the estimated regression coefficients for different soil depth and nutrient classes (Table 1). The model of below-ground fine root production of Nadelhoffer and Raich (1992) was used to estimate the mean and SD of $P_{n,yb}$,

$$P_{n,yb} = -0.07 + 0.56 P_{n,ya}. \quad (12)$$

Replacement of coarse woody tissue lost each year by mortality was calculated as a fraction of above-ground biomass lost each year, viz.

$$P_{n,yc} = \gamma B_a \quad (13)$$

where $\gamma = 0.01$ for tall, medium and low forest Vegetation Classes (AUSLIG, 1990) and $\gamma = 0.00$ for herbaceous, grass, forb, low shrub and tall shrub Vegetation Classes (AUSLIG, 1990) based on estimates from the literature. For example, above-ground biomass loss by mortality in Australian sub-tropical rainforest (Turner

Table 1. *Coefficients of the multiple linear regression model of above-ground fine tissue net primary productivity ($P_{n,ya}$) for various soil nutrient and depth classes in VAST1.0*[a]

Nutrient class	Depth class	Estimated regression coefficients	
		β_0	β_1
No data	No data	−4.70	1.45
1	No data	−7.22	1.81
2	No data	−2.07	1.09
3	No data	4.05	0.25
No data	1	−3.75	1.26
1	1	−3.75	1.26
2	1	5.22	0.07
3	1	2.28	−0.94
No data	2	−7.70	1.89
1	2	−11.46	2.46
2	2	−3.36	1.26
3	2	3.98	0.25
No data	3	−3.31	1.24
1	3	−10.69	2.29
2	3	−1.73	1.09
3	3	5.34	0.08

[a]The nutrient classes are: 1, 2 and 3 for low, moderate and high nutrient values, respectively; and three depth classes are: 1, 2 and 3 for a soil depth of 0.0–0.5, 0.5–1.5 and >1.5 m, respectively. Where data of soil nutrient status or soil depth are not available, regression coefficients for "no data" class were used.

et al., 1989) and Victorian *Eucalyptus obliqua* forests (Attiwill, 1979) each year is about 1% and 2%, respectively. For calculating the SD of $P_{n,yc}$, we assumed that the coefficient of variation (CV), defined as the ratio of standard deviation and mean for $P_{n,yc}$, was equivalent to the CV of above-ground NPP.

Predicted above-ground biomass, B_a, was obtained from another statistical model developed by Barrett et al. (2001):

$$\ln(B_a) = -33.19 + \beta_2 + 6.52\ln(x_R) + 0.933(x_T) - 0.1578[\ln(x_R)x_T] \quad (14)$$

where x_T is mean annual temperature (°C), and β_2 varies with soil nutrient class only, and is equal to 0.0, 0.26 and 0.10 for soil nutrient Class 1, 2 and 3, respectively.

Overall the VAST1.0 model accounts for 69% of the variance in the 183 NPP observations. All dependent and independent variables were log-transformed in the statistical models. This was to ensure homogeneity of the residual variance.

The variance of total annual NPP was estimated by summing up the variance and covariance of its three components. The correlation coefficient between every two of three different components is assumed to be 0.9 in the absence of further information and as a reasonable starting position. The justification for a high value of correlation coefficient is that we expect ecosystem components to co-vary across the landscape (e.g. high above-ground NPP is likely to be associated with high below-ground NPP). Where this assumption is in error, it is likely to overestimate, rather than underestimate, the SD of annual NPP of the above-ground coarse tissue.

The estimated annual mean NPP and its SD for each 5 km by 5 km grid box represent the values expected for a relatively undisturbed ecosystem for which the net carbon flux integrated over a whole year is zero. VAST1.0 partitions total variance in the observations into systematic and random terms. Spatial interpolation of NPP at a 5 km by 5 km resolution for the continent is achieved using the statistical model and continental datasets of auxiliary variables (climate, vegetation and soils) in a geographic information system (ArcView, Environmental Systems Research Institute, Redlands, Ca., USA). The SD of predicted annual mean NPP for each grid cell was also obtained from the statistical models. Figure 1 shows the mean and SD of annual mean NPP of the Australian continent predicted by VAST1.0. The NPP in the south-east coastal region and northern part generally is above 400 gC m^{-2} yr^{-1}, and is less than 200 gC m^{-2} yr^{-1} in the central and north-west part of the continent, reflecting the spatial variation of annual rainfall and air temperature.

Not all of the climatic range of Australia was covered by the observed data of NPP and unbiased predictions for those areas using VAST1.0 were not possible (and so appear as blanks in Fig. 1). This excluded an area of 2.2% (approximately 170000 km^2) of the continent from the analysis. Using the vegetation type map of the Australian continent (R.D. Graetz, unpublished data) and the estimates of the mean and SD of NPP for 97.8% of the continent by VAST1.0, we calculated the mean and SD of NPP of each vegetation type, which were then used to provide the estimates of the mean and SD of NPP of the same vegetation type of the grid boxes where VAST1.0 is not applicable (Fig. 1). This represents our best estimates for those 2.2% of the Australian continent.

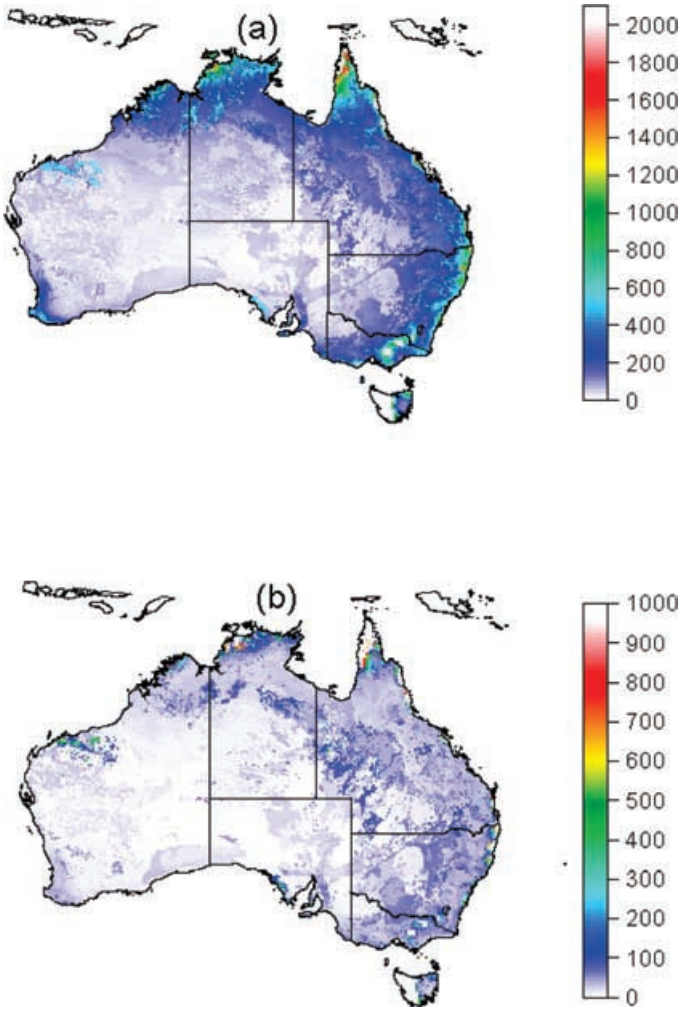

Fig. 1. Estimated annual mean net primary production (a) (gC m^{-2} y^{-1}) and its standard deviation (b) (gC m^{-2} y^{-1}) for every 5 km by 5 km grid box by VAST1.0. VAST1.0 is not applicable in four regions in white in south-east Australia and Tasmania. Boundaries of six states and Northern Territory in Australia are also shown.

The mean annual NPP at 5 km by 5 km resolution was then aggregated to give the estimated mean NPP at 75 km by 75 km spatial resolution as for the atmospheric transport model. Aggregation of the variance of annual mean NPP from 5 km by 5 km to that at 75 km by 75 km spatial resolution requires knowledge about the spatial and temporal correlations of the NPP at the finer resolution. This is discussed next.

2.3. Propagating error of the estimated mean NPP into the errors of estimated monthly mean carbon fluxes

To estimate the SD of monthly mean of gross photosynthesis, and plant and soil respiration at 75 km by 75 km spatial resolution, we first calculated the SD of annual mean NPP at 75 km by 75 km. From this, we calculated the SD of annual mean of gross

photosynthesis, plant or soil respiration. The SD of monthly mean carbon flux was then estimated using the temporal correlation of monthly carbon fluxes and the SD of the annual mean carbon fluxes at 75 km by 75 km resolution.

To estimate the variance of annual NPP ($\sigma^2_{\mathrm{n,y}}$) for each 75 km by 75 km grid box of the Australian continent, we summed the variance and covariance estimated by VAST 1.0 of all 225 5 km by 5 km grid boxes that comprise each 75 km by 75 km CBM grid box. That is

$$\sigma^2_{\mathrm{n,y}} = N\left(\frac{P_{\mathrm{n,y}}}{\overline{P_{\mathrm{n,y}}}}\right)^2 \sum_i \sum_j \rho_{i,j}\sigma^*_{\mathrm{n,y}}(i)\sigma^*_{\mathrm{n,y}}(j) \qquad (15)$$

where $\rho_{\mathrm{i,j}}$ is the spatial autocorrelation of the estimates of NPP between the ith $[\sigma^*_{\mathrm{n,y}}(i)]$ and jth $[\sigma^*_{\mathrm{n,y}}(j)]$ cells at the 5 km by 5 km spatial resolution in VAST1.0 and $N = 9$ for the study period of 1990–1998. The spatial variation of NPP depends on climate, soil condition, vegetation properties and disturbance, all of which are spatially correlated. Therefore covariance must be included in calculating the SD of NPP for the 75 km by 75 km grid boxes from the estimates of SD at 5 km by 5 km grid boxes, otherwise the SD of NPP at 75 km by 75 km grid boxes will be significantly underestimated.

Because of insufficient data it is not possible to construct a variogram of the spatial correlation of NPP to estimate $\rho_{i,j}$. Instead we used Moran's I statistic (Cliff and Ord, 1981) to construct a simple correlogram of spatial correlation of NPP as a function of distance between NPP data points. We then approximated the shape of the correlogram with an exponential model of spatial autocorrelation of the form

$$\rho_{i,j} = k_1 \exp(-k_2 x) \qquad x > 0 \qquad (16)$$

$$\rho_{i,j} = 1 \qquad x = 0, \qquad (17)$$

where x is the distance between grid cells i and j (km); for the present work $k_1 = 0.7$ and $k_2 = 0.0045$ km^{-1}. In this way information on the covariance of NPP from ecological observations was used to calculate the SD of estimated annual mean NPP at the 75 km by 75 km resolution for the Australian continent.

The SDs of the annual mean of gross photosynthesis, plant or soil respiration, $\sigma_{\mathrm{g,y}}$, $\sigma_{\mathrm{a,y}}$ and $\sigma_{\mathrm{s,y}}$, were calculated using the following assumptions:

$$\sigma^2_{\mathrm{g,y}} = \sigma^2_{\mathrm{a,y}} = 0.5\sigma^2_{\mathrm{n,y}} \qquad (18)$$

$$\sigma^2_{\mathrm{s,y}} = \sigma^2_{\mathrm{n,y}}. \qquad (19)$$

The SD of annual mean net ecosystem production, $\sigma_{\mathrm{e,y}}$, was then calculated as

$$\sigma_{\mathrm{e,y}} = \sqrt{\sigma^2_{\mathrm{n,y}} + \sigma^2_{\mathrm{s,y}}} = \sqrt{2}\sigma_{\mathrm{n,y}}. \qquad (20)$$

Here we assume that the annual GPP, autotrophic respiration and heterotrophic respiration are uncorrelated because of lack of measurements.

To relate SD of monthly mean carbon flux to the SD of its annual mean, we constructed a first-order autoregressive error model (see Appendix). The first-order error model was used to relate the SD of monthly mean P_{g}, R_{a} and R_{s} to their respective SD of the annual mean for every grid cell (75 km by 75 km) for the Australian continent.

2.4. *Estimating three key model parameters:* J_{max}, r_p *and* r_s

CBM calculates the exchanges of water, heat and CO_2 between the land surface and atmosphere for given inputs of land surface parameters and meteorological inputs. Inputs include 25 plant and soil parameters. It is not possible to derive the estimates of all model parameters using the datasets described previously. A recent study by Wang et al. (2001) showed that fewer than four parameters in CBM could be estimated independently using measurements of hourly energy and CO_2 fluxes at crop or pasture sites in south-east Australia. Leuning et al. (1998) found that the predicted energy or CO_2 fluxes by CBM agreed well with measurements using a constant value of leaf $j_{\max}$ for the entire growing season for crops or pastures in south-east Australia. Using the estimates of annual mean NPP and monthly canopy green area index at 75 km by 75 km resolution for the Australian continent, we estimated three key parameters in CBM, $J_{\max}$, r_{p} and r_{s} as follows.

All model parameters are assumed to be constant in time. Only three parameters, $J_{\max}$, r_{p} and r_{s} in CBM are allowed to vary between grid cells. $P_{\mathrm{g,y}}$, $R_{\mathrm{f,y}}$, $R_{\mathrm{p,y}}$ and $R_{\mathrm{s,y}}$ for that grid cell in CBM are calculated as:

$$P_{\mathrm{g,y}} = f_1(\mathbf{M}, j_{\max}, L) \qquad (21)$$

$$R_{\mathrm{f,y}} = f_2(\mathbf{M}, V_{\mathrm{cmax}}) \qquad (22)$$

$$R_{\mathrm{p,y}} = r_{\mathrm{p}} f_3(\mathbf{M}) \qquad (23)$$

$$R_{\mathrm{s,y}} = r_{\mathrm{s}} f_4(\mathbf{M}, r_{\mathrm{s}}) \qquad (24)$$

where $\mathbf{M}$ represents meteorological inputs provided by DARLAM, and f_{k} (k = 1, 2, 3 or 4) represents

functions from CBM. Three parameters, j_{max}, r_p and r_s, can be estimated if $P_{g,y}$, $R_{p,y}$ and $R_{s,y}$ are known for a given $\mathbf{M}$.

As a first-order approximation, we assume that NPP/GPP = 0.5 for all land points and $\overline{P_{e,y}} = 0$, or $\overline{P_{n,y}} = -\overline{R_{a,y}} = -\overline{R_{s,y}} = 0.5\overline{P_{g,y}}$. Because of our steady-state assumption, estimates of annual NEP should be close to zero. Our objective here is to obtain reasonable estimates of carbon fluxes of photosynthesis, plant and soil respirations, which can then be used to provide prior estimates for the Bayesian synthesis inversion for the companion study (Wang and McGregor, 2003).

To estimate j_{max}, we used CBM to calculate $P_{g,y}$ for j_{max} at each of 10, 25, 50, 75, 125, and 250 μmol m^{-2} s^{-1} for each 75 km by 75 km grid box of the Australian continent. The function, $P_{g,y} = aj_{max}/(b + j_{max})$ was fitted to these data to estimate j_{max} by assuming $\overline{P_{g,y}} = 2\overline{P_{n,y}}$. The r^2 of this fit was greater the 0.99 for all grid cells. We calculated canopy J_{max} using eq. (3) and the estimate of canopy green area index, and $\overline{R_{f,y}}$ using eq. (22).

Once J_{max} is known, we can calculate $P_{g,y}$ and $R_{f,y}$ for each year. Taking an approach similar to that outlined by Denning et al. (1996), we estimated r_p and r_s using the following equations:

$$r_p = \frac{\int_{t-1} (-0.5P_g - R_f)\,dt}{\int_t f_3\,dt}, \tag{25}$$

$$r_s = \frac{\int_{t-1} -0.5P_g\,dt}{\int_t f_4\,dt}. \tag{26}$$

That is to assume that the annual totals of plant respiration and soil respiration of year t are equal to NPP of the previous year $t-1$, respectively. The estimates of r_p and r_s using eqs. (25) and (26) would vary from year to year. We found that interannual variations of r_p and r_s were less than 10% for all grid boxes of the Australian continent. This approach tends to produce less interannual variability of annual NPP and NEP for the Australian continent than if the long-term means, $0.5\overline{P_{g,y}} + \overline{R_{f,y}}$ and $0.5\overline{P_{g,y}}$, were used in estimating r_p and r_s in eqs. (25) and (26). The estimates of respiration fluxes here will be used as prior estimates for the subsequent inversion (see Wang and McGregor, 2003). We assume that r_p and r_s are time-independent within a year but vary from year to year. Therefore inversion results should not be affected significantly by either approach we use for estimating r_p and r_s, providing the prior estimates of SD of plant and soil respiration fluxes are reasonably large.

2.5. *Calculation of monthly carbon fluxes for eight land regions in the Australian continent*

The estimates of the three key parameters, j_{max}, r_p and r_s, are spatially explicit, the estimate of j_{max} is fully time independent, while the estimates of r_p and r_s may vary from year to year, but are constant within a year, as explained above. We used CBM to calculate the fluxes of gross photosynthesis, plant and soil respiration for every time step at which the meteorological inputs were provided by DARLAM (900 s). The calculations were performed for the period 1989–1998, and the annual total of gross photosynthesis for 1989 was used to estimate r_p and r_s for each grid cell of the Australian continent for year 1990 and so on. The monthly total fluxes of gross photosynthesis, plant and soil respiration were then summed up. The monthly fluxes of gross photosynthesis, plant and soil respiration were also calculated for each of the eight regions for the period 1990–1998.

3. Data

3.1. *Spatially explicit data of canopy green area index*

One of the key plant parameters in CBM is canopy green area index (L). No surface-based measurements of L exist for the entire Australian continent but the few measurements that do exist underpin plausible estimates of their range and dynamics. This understanding was used to derive estimates of L from satellite datasets that were available for the continent for 1981–1991.

The data used were from the Advanced Very High Resolution Radiometer (AVHRR) carried on the NOAA satellite series. Although not specifically designed to do so, the AVHRR sensor has provided a data stream and archive that has revolutionised our understanding of the nature and dynamics of the global land cover, e.g. De Fries et al. (1999) and Zeng et al. (2000). The AVHRR sensor acquires data in the red and near infrared, and these two channels are most frequently combined arithmetically into the Normalised Difference Vegetation Index (NDVI) that has become very widely used, e.g. Sellers et al.

(1994). Because it exploits the difference in red and near-infrared reflectance, the NDVI is a direct measure of canopy greenness, and therefore indirectly a measure of total (green plus non-green) canopy variables. Gutman and Ignatov (1998) first derived an estimate of L from NDVI data, and their methodology was followed here. The NDVI dataset used was ex-NASA (C.J. Tucker, personal communication), monthly resolution, 1981−1991, heavily edited for non-surface artefacts. Following the methodology of Gutman and Ignatov (1998), only two expert decisions were required: the maximum L, set as 5, and the NDVI value for bare soil, set as 0.02. The use of these two values resulted in an annual climatology of 5 km by 5 km, monthly L values (Fig. 2).

3.2. Data for developing and calibrating VAST1.0

Barrett (2001) compiled 183 field measurements of NPP for steady-state ecosystems in Australia from the scientific literature. A description of data compilation methods and data coverage was given in part in Barrett et al. (2001) and Barrett (2001). Only a brief description is given here. These NPP data and the associated data of annual rainfall, annual mean air temperature, soil nutrient status and vegetation types were used to calibrated a statistical model, VAST (Vegetation And Soil-carbon Transfer) 1.0. The calibrated VAST1.0 was then used to estimate the mean and SD of annual NPP of every 5 km by 5 km grid cell of the Australian continent (also see section 3.2).

Observations from sites assumed to be near steady state were chosen from the published scientific literature. By stipulating that measurements had undergone scientific peer review, a level of data quality control was guaranteed. The criterion used to select steady-state sites was that the author's description of overstorey vegetation structure and species composition in the original study matched the vegetation classification for a site from the 1788 Australian Survey and Land Information Group (AUSLIG) pre-European Historical Vegetation Atlas (AUSLIG, 1990). It was assumed here that the all vegetations were at steady state before the European settlement in Australia.

Above-ground NPP was derived from either biomass increment of annual herbage, measured as change in dry mass of vegetation per unit area over time, or the measurement of litterfall accumulation in above-ground litter traps. Sample areas ranged in size from 1 m^2 quadrats for herbaceous vegetation to the application of allometric equations on forest plots of up to 0.25 ha. Litterfall measurements included a "wood fraction"; however, the maximum size of this fraction varied from 0.6 cm to 5 cm diameter between studies. Observations of above-ground NPP in the dataset ranged from 19 to 1964 g C m^{-2} yr^{-1}.

Other data used in calibrating VAST1.0 included the 0.25° Australian Bureau of Meteorology Research Centre and the National Climate Centre archive of interpolated continental climate surfaces for monthly maximum and minimum temperature and rainfall; the AUSLIG topographic map of Australia at 1:2 500 000 scale; the Australian 0.05° Digital Elevation Model developed by the Australian National University, Centre for Resource and Environmental Science, (ANU-DEM); and the digital version of the Atlas of Australian Soils at 1:2 000 000 scale. The soils atlas was combined with look-up tables developed by McKenzie and Hook (1992) to convert map unit soil classification to three "Gross Nutrient Status" classes.

3.3. Meteorological inputs for CBM

We used a regional atmospheric model, DARLAM (McGregor and Walsh, 1994), to provide the meteorological inputs to CBM. DARLAM was initialised using the European Centre for Medium-Range Weather Forecast (ECMWF) analyses. The standard 12-h, 2.5° resolution, 14-pressure-level ECMWF analyses were first horizontally interpolated to every 75 km grid point in the model domain and then interpolated to 18 vertical levels. All the meteorological fields were then updated twice daily (00:00 UTC and 12:00 UTC) at the boundary, and once daily in the interior (00:00 UTC) over the whole domain using the ECMWF data. At every integration time step in DARLAM, CBM was also used to provide the surface boundary conditions, and the advection of the calculated CO_2 fluxes from the surface by CBM was also calculated in DARLAM. See Wang and McGregor (2003) for further details about the transport of surface CO_2 emissions within the DARLAM domain. DARLAM was spun up using the interpolated ECMWF analysis data from January to December 1989, and the simulation results for the period 1990 to 1998 were used in this study. The time step for integration in DARLAM is 900 s.

It is also necessary to partition the Australian continent into eight regions (A to H) (Fig. 3) for Bayesian synthesis inversion in the companion paper (Wang and McGregor, 2003). In this paper, we use these regions as a means of comparing carbon fluxes between different parts of the continent.

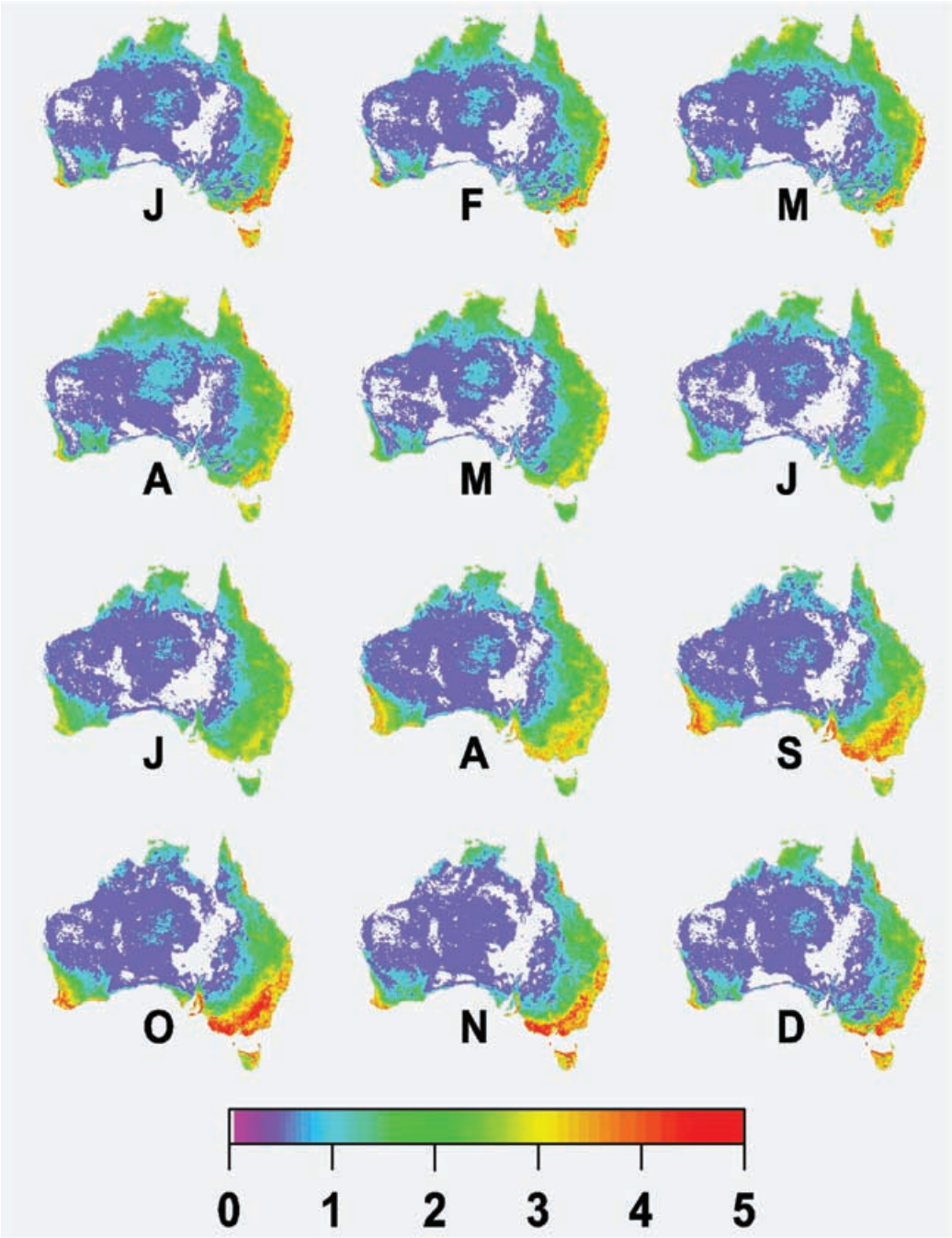

Fig. 2. Monthly canopy green area index estimated from AVHRR NDVI data from 1984–1992.

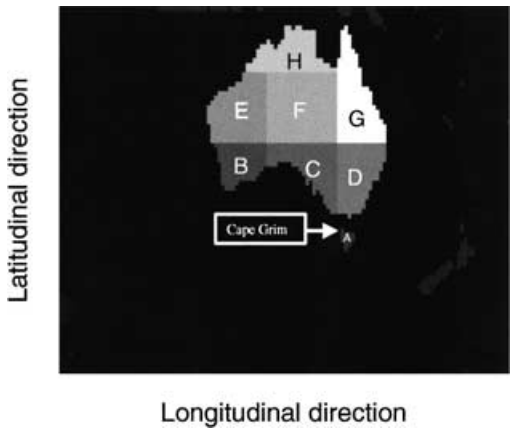

Fig. 3. The boundaries of eight land regions (A–H) in Australia. Cape Grim is located at the north-west tip of region A.

4. Results

4.1. Spatial variations of three model parameters: J_{max}, r_p *and* r_s

The spatial variation of J_{max} is similar to that of annual NPP, and generally higher along the coast than in inland regions (Fig. 4a). In central Australia, estimated J_{max} is generally less than 10 μmol m^{-2} s^{-1}, but is greater than 100 μmol m^{-2} s^{-1} in a few locations in the north-east and south-east of the mainland of Australia and in Tasmania, where tropical and temperate rainforests occur (Fig. 4a). The mean J_{max} over the entire Australian continent was 13 μmol m^{-2} s^{-1}, which is significantly lower than most grasslands worldwide and comparable to that of coniferous forests in the northern hemisphere (Wullschleger, 1993).

In a literature survey, Ferrar (1988) summarised measurements of the maximum photosynthetic rate of Australian plants. We calculated from Ferrar's (1988) data the maximum leaf potential electron transport rate, j_{max}, for different vegetation types in Australia. Lower in-situ photosynthetic capacity is to be expected because most measurements of leaf photosynthetic capacity as summarised by Ferrar (1988) are made on seedlings, or plants grown under optimal conditions. Our estimates of J_{max}/L (i.e. average canopy electron transport capacity on a leaf area basis) are much lower than Ferrar's data except for tropical rainforest in northern Australia. Our estimate of leaf j_{max} (i.e. maximum electron transport capacity of leaves at the top of the canopy) is about 40 (μmol m^{-2} s^{-1}

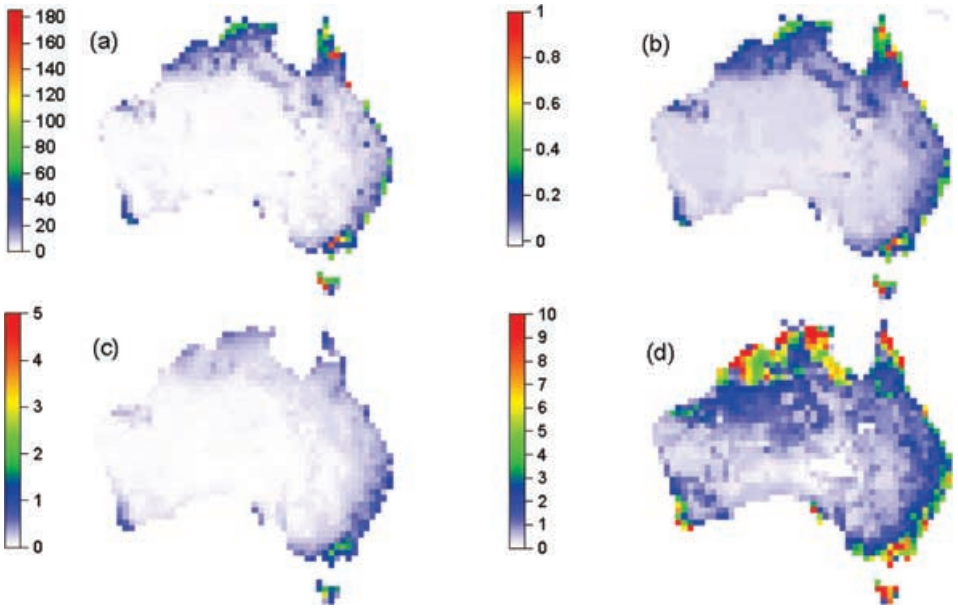

Fig. 4. The estimated (a) mean J_{max} (μmol m^{-2} s^{-1}) and (b) leaf respiration rate at 20 °C (μmol m^{-2} s^{-1}); and (c) the estimated mean non-leaf tissue plant respiration rate at 20 °C (μmol m^{-2} s^{-1}) and (d) mean soil respiration rate at 20 °C without soil water limiting (μmol m^{-2} s^{-1}) for the Australian continent at 75 km by 75 km spatial resolution.

for tropical rainforest in northern Australia, which issimilar to values from Ferrar (1988) and Eamus and Prichard (1998), but is only half as much as measurements from tropical rainforest in central Amazonia (Carswell et al., 2000). In central Australia, our estimate of J_{max}/L is less than 20 μmol m^{-2} s^{-1}, as compared with 130 ± 41 μmol m^{-2} s^{-1} for C4 grass as calculated from Ferrar's data which were based on less than 10 measurements on well watered and fertilized plants. Our estimate of J_{max}/L for temperate forests in south-east Australia is only 40 μmol m^{-2} s^{-1}, only half as much as the estimate for *Eucalyptus* leaves from Ferrar's data (Ferrar, 1988). Many factors may contribute to the difference between the two estimates, such as non-optimal growth conditions and leaf age. The average age of Eucalyptus leaves is about 2 yr, the maximum potential electron transport rate of a full size leaf decreases rapidly with leaf age for most tree species (Hanba et al., 2001). Our estimate represents the mean of maximum potential electron transport rate for all leaves within the canopy, whereas most measurements as summarised by Ferrar (1988) were made on less than 1-yr-old seedlings grown under optimal conditions.

Figures 4b and 4c show that the estimated leaf and non-leaf plant tissue respiration rate at 20 °C, $r_f + r_p$, varied between 0 and 6 μmol m^{-2} s^{-1}, and was less than 1 μmol m^{-2} s^{-1} over 90% of the continental land area. Non-leaf plant respiration rate at 20 °C, r_p was greater than 4.0 μmol m^{-2} s^{-1} for only one grid cell each in the south-east Victorian forest and in Tasmania (Fig. 4c). Our estimate of total plant (leaf and non-leaf tissue) respiration rate is comparable to that observed in tropical rainforest of Brazil after accounting for differences in canopy LAI (Lloyd et al., 1995). From measurements compiled by Ferrar (1988), we calculated that leaf respiration rates for vegetation classes at 25 °C (including one SD) were 1.7 ± 1.5 μmol m^{-2} s^{-1} for *Acacia*, 1.3 ± 0.3 μmol m^{-2} s^{-1} for *Eucalyptus* and 0.9 ± 0.5 μmol m^{-2} s^{-1} for tropical rainforests in Australia; all these rates are calculated on a leaf area basis. Our estimate of annual mean R_f is less than 0.2 μmol m^{-2} s^{-1} for most of central Australia, and about 0.2 – 0.5 μmol m^{-2} s^{-1} for coastal regions. The spatial variation of leaf or plant respiration rates is also similar to that of annual NPP. Annual leaf respiration across Australia is much smaller than non-leaf plant respiration, and accounts for less than 20% of annual total plant respiration. It is likely that respiration from fine-root turnover accounts for much of the below-ground plant respiration (Norby et al., 1992; Wang et al., 1998), and therefore is very important in determining the net carbon exchange of terrestrial ecosystems.

Figure 4d shows that the soil respiration rate at 20 °C and optimal moisture, r_s, was less than 5 μmol m^{-2} s^{-1} for most of the continent. The combined annual mean ecosystem respiration rate (R_t) varied from less than 2 μmol m^{-2} s^{-1} in central Australia to about 12 μmol m^{-2} s^{-1} in the temperate forests of south-east Australia (data not shown). Our calculations showed that annual mean total ecosystem respiration was about half the rate under optimal conditions (20 °C and non-limiting soil moisture).

Our estimates of $r_f + r_p + r_s$ are about 4 μmol m^{-2} s^{-1} for the temperate forests in south-east Australia, 6 μmol m^{-2} s^{-1} for the tropical forests in northern Australia, and 2.5 μmol m^{-2} s^{-1} for the temperate grasslands in south-east Australia. Meyer et al. (unpublished data) found that the measured total ecosystem respiration rate at 20 °C was 1.4–2.1 μmol m^{-2} s^{-1} for crops and pasture in south-east Australia, and measured below-ground respiration (soil and plant roots) was 0.4 μmol m^{-2} s^{-1} for an undisturbed mallee ecosystem, and 0.6 μmol m^{-2} s^{-1} for a temperate forest ecosystem. Taking an average leaf area index of 3 for the temperate forest during the growing season and leaf respiration rate of 0.9 μmol m^{-2} s^{-1} at 20 °C (Ferrar, 1988), the total respiration rate of the temperate forest in south-east Australia is 3.3 μmol m^{-2} s^{-1}, which is comparable to our model estimates for temperate forests of 4 μmol m^{-2} s^{-1} in this region.

4.2. Seasonal variation of carbon exchanges over the period 1990 to 1998

Figure 5 shows the monthly means and their SDs of gross photosynthesis ($P_{g,m}$), and autotrophic ($R_{a,m}$) and soil ($R_{s,m}$) respiration for each of eight regions of the Australian continent for 1992. Fluxes are highest in region A and lowest in region E, which reflect differences in the dynamics of soil water and nutrients across the continent.

There are significant differences in seasonal variation of $P_{g,m}$, $R_{a,m}$ and $R_{s,m}$ between different regions. In region A, where water is least limiting, both respiratory fluxes and gross photosynthesis are greatest in December and least in June, which suggests that air temperature and incident solar radiation are the most important limiting factors for respiration and photosynthesis in this region. In regions B–D, where winter is cool and wet, summer is hot and dry, plant growth

is limited by soil water during the Australian summer, the gross photosynthetic flux is greatest (most negative) in October and least in June or July, while respiration fluxes generally are lower in winter than summer, following the seasonal variation in air temperature.

Seasonal variation of gross photosynthesis in regions E–G is distinctly different from that in other regions (Fig. 5). Comparing with regions A–D, the dry season from May to September in regions E–G is quite cool and the wet season from October to the following April is hot and humid, with more than 15% of days having maximum temperatures over 30 °C in these three regions (Bureau of Meteorology, 1988). Therefore, gross photosynthesis is greatest (most negative) and soil respiration is least in April at the end of the wet season, and plant respiration varies

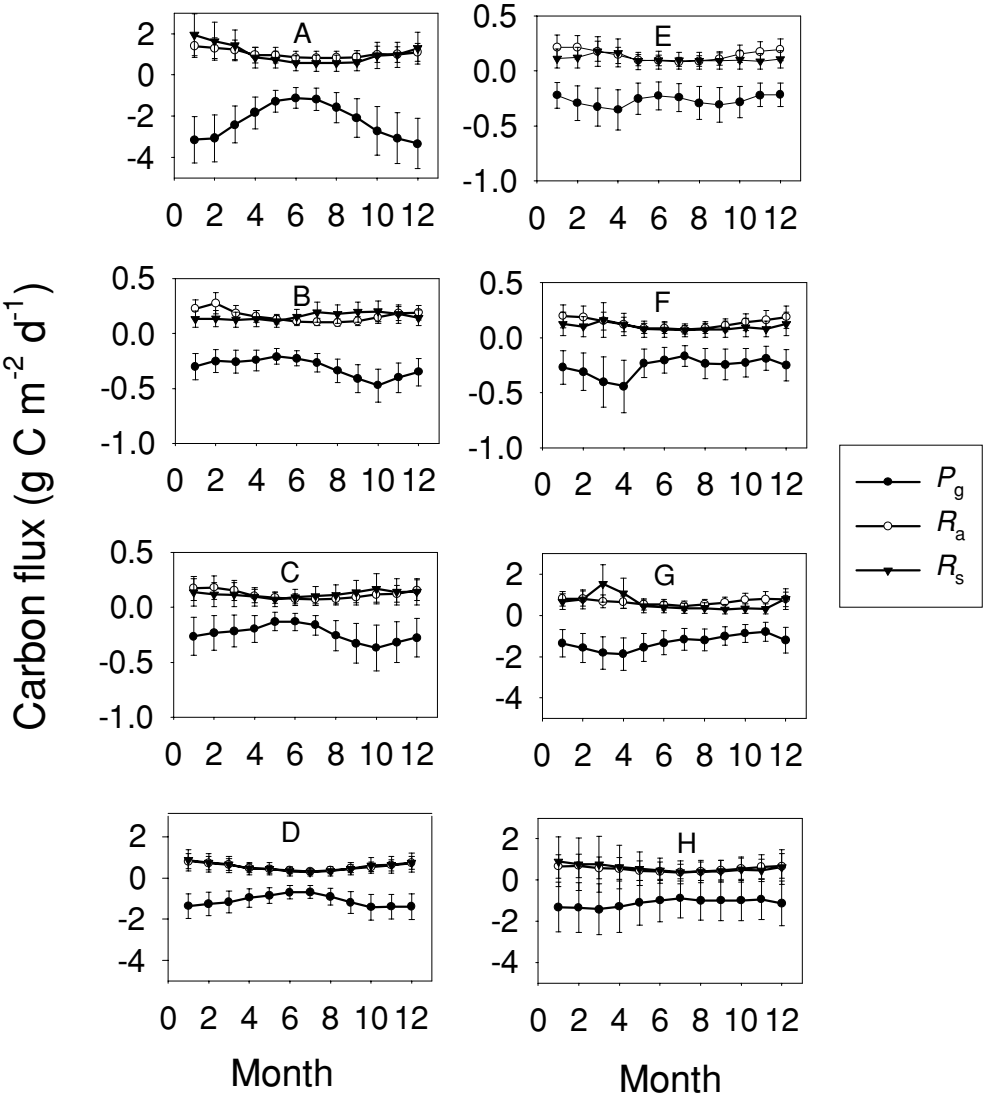

Fig. 5. Variations of monthly mean gross primary production (solid circle), plant respiration ($R_f + R_P$) (open circle) and soil respiration (triangle) and their one standard deviation for each of the eight regions in Australia in 1992. Note that two different vertical scales were used.

seasonally with air temperature. Change in plant phenology with seasonal rainfall also contributes to the seasonal variation of photosynthesis and plant respiration in these three regions.

Seasonal variation of gross photosynthesis is primarily driven by seasonal rainfall in regions G and H, and is greatest (most negative) at the end of the wet season in April. Respiratory fluxes are lowest in July. Seasonal variation of plant and soil respiration is similar in these two regions, even though the coefficient of variation (CV) is largest in region H because few measurements were available for calibrating VAST1.0 and there are larger differences in rainfall between the wet and dry seasons in region H than region G.

Seasonal variation of NPP is shown in Fig. 6 for regions A–H for the period 1990−98. The seasonal

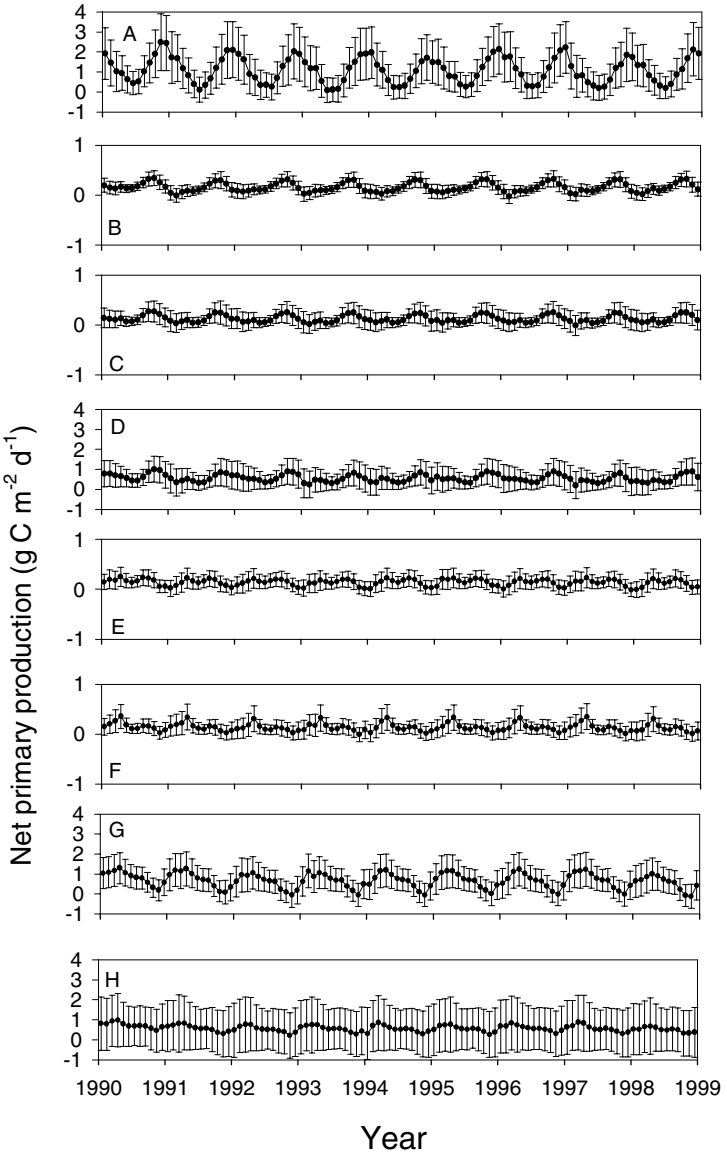

Fig. 6. Variations of monthly mean net primary production and its 1 SD for each of the eight regions from 1990–1998. Note that two different vertical scales are used.

variation of NPP is similar between years in the period 1990−98 for all eight regions. The estimate of NPP for region H has the greatest uncertainty. The mean CVs for monthly NPP for the period 1990−98 for regions A–H are 0.34, 0.30, 0.49, 0.34, 0.50, 0.50, 0.37 and 0.72.

The mean monthly NPP in regions A, D, G and H is about one order of magnitude greater than that in regions B, C, E and F because of the difference in rainfall and temperature. The NPP in the southern regions (A–D) decreases from the beginning of the year until June or July and then increases until the end of the year. The monthly NPP in the central regions (E and F) has two maxima each year, reflecting the interactive influences of temperature and rainfall on photosynthesis and respiration in the desert region of Australia (Fig. 5). The second maximum of NPP is a result of increasing rainfall and moderate air temperature at the end of the dry winter (September or October) in the desert region. In the tropical regions G and H, the monthly NPP varies with seasonal rainfall. The monthly NPP increases during the wet season (from November to April) and decreases during the dry season (from May to October).

As expected, SD of monthly NPP is larger than SD of annual NPP for all regions. In addition, since NEP is the residual of NPP and R_t, absolute and relative SDs of monthly NEP are larger than monthly NPP. Therefore the uncertainty in estimated NEP is large in all eight regions. Because of these large uncertainties, mean monthly NEP is not significantly different from zero for most months in the period 1990−98 (data not presented here).

4.3. Seasonal variations of monthly NPP and NEP of the whole Australian continent

Figure 7 shows the seasonal variation of monthly NPP and NEP of the whole Australian continent for the period 1990−98. Seasonal variation in NPP is characterised by two cycles each year. In the first cycle, minimum NPP occurs in June and the maximum NPP in April. In the second cycle, the minimum NPP occurs in November or December and the maximum in September. These dynamics result from the different seasonality of photosynthesis and plant respiration between southern and northern Australia. In southern Australia, (regions A–D) photosynthesis is greatest in October following winter rain and spring canopy growth. In northern Australia (regions E–H) photosynthesis is greatest in April at the end of the monsoon. The amplitude of the first cycle tends to be greater than that of the second cycle during the period of 1990−98. Using the method outlined by Thoning et al. (1989), we estimated that the seasonal amplitude as the difference between the maximum and minimum monthly NPP in any year varied between 44 and 64 Mt C month^{-1} during this 10-yr period, being smallest in 1998 (44 Mt C month^{-1}) and largest in 1994 (64 Mt C month^{-1}).

Seasonal variation of net ecosystem exchange, $P_{e,m}$, aggregated over all regions has two periods each year when the flux into the biosphere is maximal. The first occurs in April and the second in August or September. The amplitude of seasonal NEP variation is quite variable between different years, being largest at 108 Mt C month^{-1} in 1997 and smallest at 61 Mt C month^{-1} in 1992 (Fig. 7). The continental biosphere was a net source over the summer half year (November–March), and a sink in the winter half year (April–October), controlled primarily by the dynamics of vegetation south of about 17°S latitude (regions A–D).

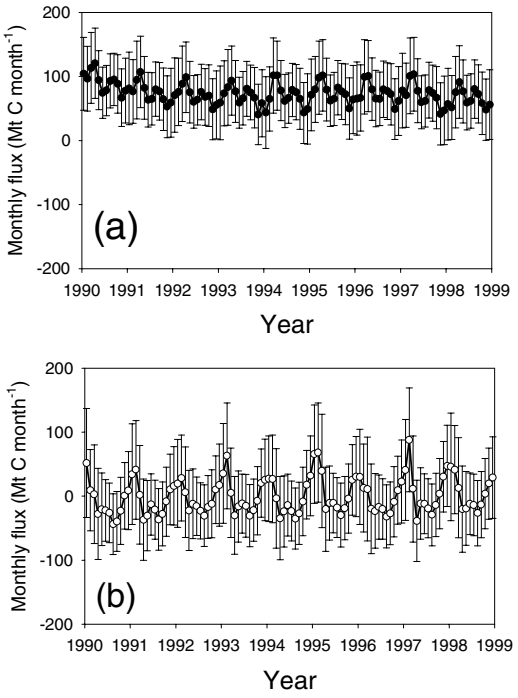

Fig. 7. Variations of monthly mean net primary production and its 1 SD (a) and monthly mean net ecosystem production and its 1 SD (b) of all terrestrial ecosystems in Australia from 1990–1998.

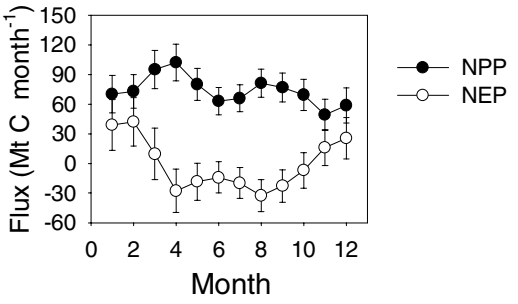

Fig. 8. Mean and one standard deviation of monthly mean net primary production (NPP) (solid circle), and net ecosystem production (NEP) (open circle) averaged over the period 1990–1998 of all terrestrial ecosystems in Australia.

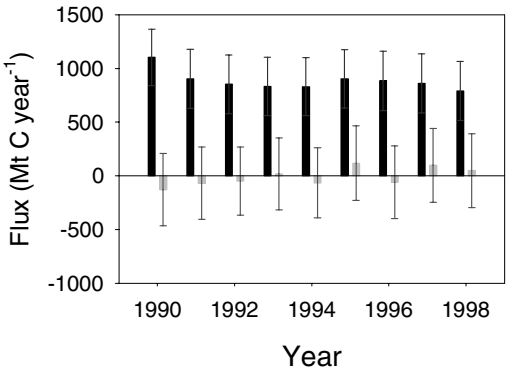

Fig. 9. Variations of annual net primary production and its 1 SD (black bar), and net ecosystem production and its 1 SD (grey bar) of all terrestrial ecosystems in Australia from 1990–1998.

The CV of monthly continental NPP estimate (Fig. 7) is about 0.68; we therefore have some confidence in predicted monthly NPP of the Australian continent by CBM. However, mean monthly NEP has a significantly larger uncertainty than NPP and we cannot predict whether in any particular month the Australian continent was a carbon sink or source using the present approach.

The mean seasonal variation averaged over 1990–1998 (Fig. 8) shows a bimodal variation of monthly mean NPP and the maintenance of a net flux into the biosphere (negative NEP) during winter for the continent as a whole. Because the SDs of monthly mean NPP or NEP between different years are assumed to be independent, the SD of the mean seasonal variation is much smaller than for months in individual years. Therefore, we are reasonably confident about the mean seasonal variation of NPP or NEP for this period. Another study (Barrett and Xu, 2003) also shows a bimodal behaviour of the seasonal NPP of the Australian continent.

4.4. Interannual variations of NPP and NEP of the whole Australian continent

The annual NPP of the Australian continent varied between 790 and 1100 Mt C yr^{-1} during the period 1990–1998 (Fig. 9). The estimate of NPP is highest in 1990 and lowest in 1998. The coefficient of variation of the modelled mean annual NPP varies from 0.24 to 0.35 for each individual year. The mean annual NPP averaged over this period was 885 Mt C yr^{-1} with a CV of 0.17.

The annual NEP of the Australian continent is much more variable than NPP (Fig. 9). Because of our steady-state assumption and the one-year lag of plant and soil respiration to NPP, we probably have significantly underestimated the interannual variation of annual NEP of the Australian continent. The terrestrial biosphere of the whole Australian continent may have been a carbon sink during 1990–1992, with a mean carbon uptake rate of 82 ± 192 Mt C yr^{-1} over that period, but may have alternated between being a carbon source and a carbon sink during the period 1993–1998. In 1995, the Australian terrestrial biosphere released 118 ± 347 Mt C yr^{-1} into the atmosphere. However, the CV of annual NEP varies between 4 and 30 for the whole Australian continent, and even the CV of annual mean NEP averaged over the whole period 1990–1998 is still 18. Therefore we cannot predict if the Australian terrestrial biosphere in aggregate was a carbon sink or source using only ecological observations and remote sensing.

5. Discussion

In this paper a method of combining information from remote sensing of canopy LAI and field measurements of NPP to constrain key parameters of CBM has been presented. We used CBM to calculate mean monthly fluxes of photosynthesis, respiration and net ecosystem exchange at 75 km by 75 km spatial resolution. Mean annual NPP of the continent varied between 800 to 1100 Mt C yr^{-1} between 1990 and 1998, with a coefficient of variation of mean annual NPP of between 0.24 and 0.34.

Our results show a bimodal variation in continental monthly mean NPP within each year due to the

different seasonality between the northern and southern parts of the continent. In northern Australia, monthly NPP increased during the wet season (from November to April) and decreased during the dry season (from May to October). In southern Australia, mean monthly NPP was greatest in October, but was limited by available soil water in the southern hemisphere summer and by low temperatures during the winter.

Predicted mean annual GPP over the period 1990 to 1998 was 787, 115, 89, 403, 98, 96, 477 and 408 gC m^{-2} yr^{-1} for regions A–G, respectively. These estimates of GPP for temperate forests, open woodlands, shrublands and grassland (regions A and D) are 20–50% of measured GPP of temperate forests in Europe and North America as reported by Valentini et al. (2000) and Falge et al. (2001). They are also significantly lower than GPP of boreal coniferous forests or cold temperate deciduous forests in Europe or North America (Falge et al., 2001). Predicted mean annual NPP between 1990 and 1998 was 404, 58, 45, 205, 50, 49, 244 and 208 gC m^{-2} yr^{-1} for regions A–G. Our estimate of NPP for region A was similar to the global mean of NPP for boreal forest, grassland and cultivated crops, but our estimates of annual NPP for regions D, G and H were generally less than published values for global annual mean NPP of woodlands and temperate forests (694 gC m^{-2} yr^{-1}: Amthor et al., 1998), and tropical forests (913 gC m^{-2} yr^{-1}). The lower NPP for Australian forests than global average may result from lower rainfall and nutrient availability, particularly phosphorus. However, the global annual mean NPP of desert and semidesert scrubs is 66 gC m^{-2} yr^{-1}, similar to our estimates of NPP in regions E and F in Australia.

Field data used for calibrating the VAST1.0 model are not distributed uniformly among vegetation classes across the continent (Barrett, 2001), and this may be a source of bias in predicted NPP. However, it is difficult to assess any bias without more field data from under-sampled regions. For example, other modelling studies suggest that VAST1.0 overestimates NPP of the northern tropical regions G and H (Raupach et al., 2001; Barrett and Xu, 2003), which is also reflected in the large prediction errors for NPP in these regions (Fig. 6). Plant growth is directly influenced by the amount of available soil water, which depends on annual rainfall and runoff. When annual runoff is relatively small, as is the case for much of Australia, annual rainfall is a reasonable surrogate for annual soil water availability. VAST1.0 can be used to provide a reasonable estimate of annual NPP because mostly runoff is small. When runoff is a significant fraction of annual rainfall, such as in coastal regions in G or H, VAST1.0 will overestimate NPP because available soil water will be significantly less than rainfall. NPP contributions from regions G and H to the continental total are about 26 and 32%, respectively. Our estimate of mean NPP over the period 1990–1998 varies from 0.8 to 1.1 Gt C yr^{-1} with a CV of 0.24 to 0.34. If we halve the NPP estimates by VAST1.0 for regions G and H, our estimate of mean annual NPP of the whole Australian continent is reduced to 0.7 Gt C yr^{-1}, which is consistent with recent estimates of 0.684 Gt yr^{-1} by Barrett and Xu (2003), but is significantly less than other estimates, e.g. 1.6 Gt C yr^{-1} (Kirschbaum, 1999b), 2.0 Gt C yr^{-1} (Field et al., 1998), 2.7 Gt C yr^{-1} (Pittock and Nix, 1986), 2.8 Gt C yr^{-1} (Gifford et al., 1992), 3.2 Gt C yr^{-1} (Roderick et al., 2001). Given the likely overestimation due to spatial bias towards more productive regions, an estimate of over 1.5 Gt C yr^{-1} for the Australian continent is outside the 95% confidence interval of our estimate, and is inconsistent with data from field measurements across Australia.

The estimates of annual NEP are much less certain than estimates of annual NPP. Our results showed that the CV of monthly mean NPP for the Australian continent varied from 0.43% to 1.28, and the CV of monthly mean NEP was greater than 4. Therefore, confidence in the predicted NEP of regions or the whole continent in any month between 1990 and 1998 was low. The uncertainty of the estimated mean carbon flux also increases with an increase in the spatial and temporal resolution. For example, the estimated annual NPP of the Australian continent is 861 ± 276 Mt C yr^{-1} with a CV of 0.32, and CV of monthly NPP of the Australian continent varies from 0.55 to 1.17 in 1997. The CV of annual NPP varies from 0.43 to 2.68 for the eight regions in 1997. Because direct measurements of carbon fluxes over a region or the whole continent are not available yet in Australia, and many factors, such as land use change, have not been considered in our modelling, confirmation of our results awaits direct measurements. On the other hand, measurements of CO_2 concentration change in space and time can provide estimates of net carbon fluxes from the land surface, as is done in global carbon studies. In the companion paper, we shall apply the Bayesian synthesis inversion to the hourly in-situ surface CO_2 concentrations measured at Cape Grim, in north-west Tasmania, Australia to improve the estimates of carbon fluxes from different regions as presented here.

6. Acknowledgements

We thank Drs Ray Leuning, Rachel Law and Belinda Medlyn for many useful discussions, and Mr Simon Bentley for developing the error model in Appendix I. We are also grateful for financial support by the Australian Greenhouse Office to the CSIRO Biospheric Working Group and by the Australian government to the CRC for Greenhouse Gas Accounting. We thank Dr L. P. Steele for providing the Cape Grim atmospheric CO_2 data.

7. Appendix. An error model for relating the SD of monthly mean carbon flux to the SD of its annual mean

To estimate the SD of the monthly mean carbon flux, we use the following error model:

$$C_m = \mu_m + \delta_m \tag{A1}$$

$$\delta_m = \beta\delta_{m-1} + \epsilon_m \tag{A2}$$

where C_m is the monthly carbon flux, and has a mean of μ_m and residual of δ_m. $m = 0, 1, \ldots 11$ for month January, February, ... December. The residual, δ_m has a zero annual mean, and is correlated with the residual at the previous time step, $m - 1$. ε_m is an independent normally distributed variable with zero mean and SD of σ_m.

By recurrence upon eq. (A2), we have

$$\begin{aligned}\delta_m &= \beta\delta_{m-1} + \epsilon_m \\ &= \beta^r\delta_{m-r} + \beta^{r-1}\epsilon_{m-r+1} + \cdots + \beta\epsilon_{m-1} + \epsilon_m.\end{aligned} \tag{A3}$$

Therefore

$$\begin{aligned}\sum_{m=0}^{11}\delta_m &= \delta_0 + (\beta\delta_0 + \epsilon_1) + \left(\beta^2\delta_0 + \beta\epsilon_1 + \epsilon_2\right) \\ &\quad + \cdots + \left(\beta^{11}\delta_0 + \cdots + \epsilon_{11}\right) \\ &= \frac{1}{1-\beta}\left[\beta(1-\beta^{12})\delta_{-1} + (1-\beta^{12})\epsilon_0\right. \\ &\quad \left. + \cdots + (1-\beta)\epsilon_{11}\right].\end{aligned} \tag{A4}$$

Since all ϵ_m are independent of each other, the variance of annual total carbon flux, σ_y^2 can be expressed as

$$\begin{aligned}\sigma_y^2 &= \mathrm{var}\left(\sum_{t=0}^{11}\delta_m\right) \\ &= \frac{1}{(1-\beta)^2}\left[\beta^2(1-\beta^{12})^2\mathrm{var}(\delta_{-1})\right. \\ &\quad \left. + \sum_{m=0}^{11}(1-\beta^{12-m})^2\mathrm{var}(\epsilon_m)\right].\end{aligned} \tag{A5}$$

To calculate $\mathrm{var}(\delta_{-1})$, we apply eq. (A3) to k years back from $m = 0$, and then sum up all the terms for the same month, and then sum up the contribution of variance of all 12 months to $\mathrm{var}(\delta_{-1})$. We have

$$\begin{aligned}\mathrm{var}(\delta_{-1}) &= \beta^{24k}\mathrm{var}(\delta_{-12k-1}) \\ &\quad + \sum_{m=0}^{11}\frac{\beta^{2(11-m)}(1-\beta^{24k})}{1-\beta^{24}}\mathrm{var}(\epsilon_m).\end{aligned} \tag{A6}$$

As $k \to \infty$, both the first term in eq. (A6) approaches zero, therefore σ_y^2 can be expressed as

$$\begin{aligned}\sigma_y^2 &= \frac{1}{(1-\beta)^2}\sum_{m=0}^{11}\left[\frac{(1-\beta^{12})\beta^{(24-2m)}}{1+\beta^{12}}\right. \\ &\quad \left. + (1-\beta^{12-m})^2\right]\sigma_m^2.\end{aligned} \tag{A7}$$

In eq. (A7), there are twelve unknowns, σ_m, $m = 0$, 11. To estimate σ_m from the estimates of σ_y and β, we assume that the coefficient of variation of the monthly carbon flux, θ, is constant within a year. Rearranging eq. (A7), we have

$$\theta = \frac{(1-\beta)\,\sigma_y}{\sqrt{\sum_{m=0}^{11}\left[\frac{(1-\beta^{12})\beta^{(24-2m)}}{1+\beta^{12}} + (1-\beta^{12-m})^2\right]\mu_m^2}}. \tag{A8}$$

By definition, we have

$$\sigma_m = \theta\mu_m. \tag{A9}$$

REFERENCES

Amthor, J. S. and members of the Ecosystems Working Group. 1998. *Terrestrial Ecosystem Responses to Global Change: a research strategy*. ORNL Technical Memorandum 1998/27, Oak Ridge National Laboratory, Oak Ridge, Tennessee, 37 pp.

Attiwill, P. M. 1979. Nutrient cycling in a *Eucalyptus obliqua* (L'Hérit.) forest. III Growth, biomass, and net primary production. *Austr. J. Bot.* **27**, 439–458.

AUSLIG 1990. *Atlas of Australian resources*. Third Series,

Volume 6, Australian Surveying and Land Information Group, Canberra, Australia.

Barrett, D. J. 2001. *NPP Multi-Biome: VAST calibration data, 1965–1998*. Available on-line [http://www.daac.ornl.gov/] from Oak Ridge National Laboratory Distributed Active Archive Research Center, Oak Ridge Tennessee, USA.

Barrett, D. J. and Xu, H. Y. 2003. Parameterisation of a large-scale terrestrial carbon cycle model by a constrained genetic algorithm using multiple data sets of ecological observations from minimally disturbed sites. *Global Biogeochem. Cycles*, in press.

Barrett, D. J., Galbally, I. E. and Graetz, R. D. 2001. Quantifying uncertainty in estimates of C-emissions from aboveground biomass due to historical land-use change to cropping in Australia. *Global Change Biol.* **7**, 833–902.

Biraud, S., Ciais, P., Ramonet, M., Simmonds, P., Kazan, V., Monfray, P., O'Doherty, S., Spain, T. G. and Jennings, S. G. 2000. European greenhouse gas emissions estimated from continuous atmospheric measurements and radon-222 at Mace Head, Ireland. *J. Geophys. Res.* **105**, 1351–1366.

Bureau of Meteorology, 1988. *Climatic averages Australia*. Australian Government Publishing Service, Canberra, Australia.

Carswell, F. E., Wandelli, E. V., Bonates, L. C. M., Kruijt, B., Barbosa, E. M., Nobre, A. S., Grace, J. and Jarvis, P. G. 2000. Photosynthetic capacity in a central Amazonia rainforest. *Tree Physiol.* **20**, 179–186.

Cliff, A. D. and Ord, J. K. 1981. *Spatial processes: models and applications*. Pion Ltd, London, UK. 266 pp.

Cramer, W., Kicklighter, D. W., Bondeau, A. and coauthors. 1999. Comparing global models of terrestrial net primary productivity (NPP): overview and key results. *Global Change Biol.* **5**, 1–15.

De Fries, R. S., Townshend, J. R. G. and Hansen, M. C. 1999. Continuous fields of vegetation characteristics at the global scale at 1-km resolution. *J. Geophys. Res.* **104**, 16911–16923.

Denning, A. S., Collatz, J. G., Zhang, C., Randall, D. A., Berry, J. A., Sellers, P. J., Colello, G. D. and Dazlich, D. A. 1996. Simulations of terrestrial carbon metabolism and atmospheric CO_2 in a general circulation model. Part I: Surface carbon fluxes. *Tellus* **48**, 521–542.

Eamus, D. and Prichard, H. 1998. A cost-benefit analysis of leaves of four Australian savanna species. *Tree Physiol.* **18**, 537–545.

Falge, E., Baldocchi, D., Tenhunen, J. and coauthors. 2001. Gap filling strategies for defensible annual sums of net ecosystem exchange. *Agric. For. Meteorol.* **107**, 43–49.

Farquhar, G. D. and von Caemmerer, S. 1982. Modelling of photosynthetic response to environmental conditions. In: *Physiological plant ecology II: water relations and carbon assimilation*, Encyclopedia of Plant Physiology, New Series, Vol 12B (eds. O. L. Lange, P. S. Nobel, C. B. Osmond and H. Ziegler). Springer-Verlag, Berlin, 549–587.

Ferrar, P. J. 1988. *Bibliography of Australian native plants. Part I. Photosynthetic responses*. Research School of Biological Sciences, Australian National University, 81 pp.

Field, C. B., Randerson, J. T. and Malmström, C. M. 1995. Global net primary production: combining ecology and remote sensing. *Remote Sensing Environ.* **51**, 74–88.

Field, C. B., Behrenfeld, M. J., Randerson, J. T. and Falkowski, P. 1998. Primary production of the biosphere: integrating terrestrial and oceanic components. *Science* **281**, 237–239.

Gifford, R. M., Cheney, N. P., Noble, J. C., Russell, J. S., Wellington, A. B. and Zammit, C. 1992. Australian land use, primary production of vegetation and carbon pools in relation to atmospheric carbon dioxide concentration. In: *Australia's renewable resources: sustainability and global change* (eds. R. M. Gifford and M. M. Barson). Bureau of Rural Resources Proceedings No. 14, Australian Government Publishing Service, Canberra, Australia, 151–187.

Gutman, G. and Ignatov, A. 1998. The derivation of the green vegetation fraction from NOAA/AVHRR data for use in numerical weather prediction models. *Int. J. Remote Sensing* **19**, 1533–1543.

Hanba, Y. T., Miyazawa, S., Kogami, H. and Terashima, I. 2001. Effects of leaf age on internal CO_2 transfer conductance and photosynthesis in tree species having different types of shoot phenology. *Austr. J. Plant Physiol.* **28**, 1075–1084.

IPCC, 1996. *Climate change 1995: the science of climate change*. Cambridge University Press, UK, 572 pp.

Kirschbaum, M. U. F. 1999a. The effect of climate change on forest growth in Australia. In: *Impacts of global change on Australian temperate forests* (eds. S. M. Howden and J. T. Gorman). Bureau of Resources Science Working Paper Series No 99/08, Canberra, Australia, 62–68.

Kirschbaum, M. U. F. 1999b. CenW, a forest growth model with linked carbon, energy, nutrient and water cycles. *Ecol. Mod.* **181**, 17–59.

Kowalczyk, E. A., Garratt, J. R. and Krummel, P. B. 1994. *Implementation of a soil-canopy scheme into the CSIRO GCM–regional aspects of the model response*. CSIRO Division of Atmospheric Research technical paper, no. 32, Melbourne, 59 pp.

Leuning, R. 1990. Modeling stomatal behaviour and photosynthesis of Eucalyptus grandis. *Austr. J. Plant Physiol.* **17**, 159–175.

Leuning, R. 1998. Scaling to a common temperature improves the correlation between the photosynthesis parameter J_{max} and V_{cmax}. *J. Exp. Bot.* **48**, 345–347.

Leuning, R., Kelliher, F. M., DePury, D. G.G. and Schultz, E. D. 1995. Leaf nitrogen, photosynthesis, conductance and transpiration: scaling from leaves to canopies. *Plant, Cell and Environ.* **18**, 1183–1200.

Leuning, R., Dunin, F. X. and Wang, Y. P. 1998. A two-leaf model for canopy conductance, photosynthesis and partitioning of available energy. II. Comparison with measurements. *Agric. For. Meteorol.* **91**, 113–125.

Lloyd, J., Grace, J., Miranda, A. C., Meir, P., Wong, S. C., Miranda, H. S., Wright, I. R., Gash, J. H.C. and McIntyre, J. 1995. A simple calibrated model of Amazon rainforest productivity based on leaf biochemical properties. *Plant, Cell Environ.* **18**, 1129–1145.

McGregor, J. L. and Walsh, K. J. 1994. Climate change simulations of Tasmanian precipitation using multiple nesting. *J. Geophys. Res.* **99**, 20889–20905.

McKenzie, N. and Hook, J. 1992. *Interpretations of the Atlas of Australian Soils*. Consulting Report to the Environmental Resources Information Network, Tech. Rep. 94/1992. CSIRO, Division of Soils, Canberra, Australia.

Nadelhoffer, K. J. and Raich, J. W. 1992. Fine root production estimates and belowground carbon allocation in forest ecosystems. *Ecology* **73**, 1139–1147.

Norby, R. J., Gunderson C. A., Wullschledger S. D., O'Neil, E. G. and McCracken, M. K. 1992. Productivity and compensatory responses of yellow-poplar trees in elevated CO_2. *Nature* **354**, 322–324.

Pittock, A. B. and Nix, H. A. 1986. The effect of changing climate on Australian biomass production–a preliminary study. *Clim. Change* **8**, 243–255.

Raupach, M. R. 1998. Influences of local feedbacks on land-air exchange of energy and carbon. *Global Change Biol.* **4**, 477–494.

Raupach, M. R., Kirby, M., Barrett, D. J. and Briggs, P. 2001. *Balances of water, carbon, nitrogen and phosphorus in Australian landscapes*. CSIRO Land and Water Technical Report 40/01, December 2001. 39 pp.

Roderick, M. L., Farquhar, G. D., Berry, S. L. and Noble, I. R. 2001. On the direct effect of clouds and atmospheric particles on the productivity and structure of vegetation. *Oecologia* **129**, 21–30.

Sellers, P. J., Tucker, C. J., Collatz, G. J., Los, S. O., Justice, C. O., Dazlich, D. A. and Randall, D. A. 1994. A global 1 degrees-by-1 degrees NDVI data set for climate studies. 2. The generation of global fields of terrestrial biophysical parameters from the NDVI. *Int. J. Remote Sensing* **15**, 3519–3545.

Tans, P. P., Fung, I. Y. and Takahashi, T. 1990. Observational constraints on the global atmospheric carbon dioxide budget. *Science* **247**, 1431–1438.

Thoning, K. W., Tans, P. P. and Komhyr, W. D. 1989. Atmospheric carbon dioxide at Mauna Loa Observatory, 2. Analysis of the NOAA/GMCC data, 1974–1985. *J. Geophys. Res*. **94**, 8549–8565.

Turner, J., Lambert, M. J. and Kelly, J. 1989. Nutrient Cycling in a New South Wales subtropical rainforest: organic matter and phosphorus, *Ann. Bot*. **63**, 635–642.

Valentini, R., Matteucci, G., Dolman, A. J. and coauthors. 2000. Respiration as the main determinant of carbon balance in European forests. *Nature* **404**, 861–865.

Wang, Y. P. and McGregor, J. L. 2003. Estimating regional terrestrial carbon fluxes for the Australian continent using a multiple-constraint approach: II. Atmospheric constraint. *Tellus* **55B** (this issue).

Wang, Y. P. and Leuning, R. 1998. A two-leaf model for canopy conductance, photosynthesis and partitioning of available energy. I. Model description and comparison with a multi-layered model. *Agric. For. Meteorol.* **91**, 89–111.

Wang, Y. P., Rey, A. and Jarvis, P. G. 1998. Carbon balance of young birch trees grown in ambient and elevated atmospheric CO_2 concentrations. *Global Change Biol.* **4**, 797–807.

Wang, Y. P., Leuning, R., Cleugh, H. A. and Coppin, P. A. 2001. Parameter estimation in surface exchange models using non-linear inversion: how many parameters can we estimate and which measurements are most useful? *Global Change Biol.* **7**, 495–510.

Waring, R. H., Landsberg, J. J. and Williams, M. 1997. Net primary production of forests: a constant fraction of gross primary production. *Tree Physiol.* **18**, 129–134.

Wullschledger, S. D. 1993. Biochemical limitation to carbon assimilation in C_3 plants–a retrospective analysis of the A/C_i curves from 109 species. *J. Exp. Bot.* **44**, 907–920.

Zeng, X. B., Dickinson, R. E., Walker, A., Shaikh, M., Defries, R. S. and Qi, J. G. 2000. Derivation and evaluation of global 1-km fractional vegetation cover data for land modeling. *J. Appl. Meteorol.* **39**, 826–839.